SCIENTIFIC NOTE ESA SN-124

September 1976

CARBON DIOXIDE AS WORKING GAS FOR LABORATORY PLASMAS

by

*R. Kist**

Institut für Physicalische Weltraum forschung

Freiburg, West Germany

(**ESRO Fellow at University of Texas in 1974*)

EUROPEAN SPACE AGENCY

AGENCE SPATIALE EUROPEENNE

ESA SN-124
Agence Spatiale Européenne
KIST, R. (Institut f. Phys. Weltraumforschung, Freiburg)
Le gaz carbonique comme source de plasmas au laboratoire.
Septembre 1976
iv + 20 pages, 16 figures. En anglais.

Des mesures ont été faites à l'aide d'une sonde HF, d'un analyseur à potentiel de freinage et d'un spectromètre de masse dans une enceinte à plasma en utilisant tour à tour du gaz carbonique, de l'azote, de l'argon et de l'hélium afin de comparer les caractéristiques de ces divers gaz pour l'obtention de plasmas en laboratoire. Dans l'ensemble, on constate que le gaz carbonique donne de plus fortes densités de plasma à de plus faibles pressions de gaz neutre en même temps qu'une plus grande composante maxwellienne de la population électronique, avec une température électronique moindre.

88

ESA SN-124
Agence Spatiale Européenne
KIST, R. (Institut f. Phys. Weltraumforschung, Freiburg)
Le gaz carbonique comme source de plasmas au laboratoire.
Septembre 1976
iv + 20 pages, 16 figures. En anglais.

Des mesures ont été faites à l'aide d'une sonde HF, d'un analyseur à potentiel de freinage et d'un spectromètre de masse dans une enceinte à plasma en utilisant tour à tour du gaz carbonique, de l'azote, de l'argon et de l'hélium afin de comparer les caractéristiques de ces divers gaz pour l'obtention de plasmas en laboratoire. Dans l'ensemble, on constate que le gaz carbonique donne de plus fortes densités de plasma à de plus faibles pressions de gaz neutre en même temps qu'une plus grande composante maxwellienne de la population électronique, avec une température électronique moindre.

88

ESA SN-124
Agence Spatiale Européenne
KIST, R. (Institut f. Phys. Weltraumforschung, Freiburg)
Le gaz carbonique comme source de plasmas au laboratoire.
Septembre 1976
iv + 20 pages, 16 figures. En anglais.

Des mesures ont été faites à l'aide d'une sonde HF, d'un analyseur à potentiel de freinage et d'un spectromètre de masse dans une enceinte à plasma en utilisant tour à tour du gaz carbonique, de l'azote, de l'argon et de l'hélium afin de comparer les caractéristiques de ces divers gaz pour l'obtention de plasmas en laboratoire. Dans l'ensemble, on constate que le gaz carbonique donne de plus fortes densités de plasma à de plus faibles pressions de gaz neutre en même temps qu'une plus grande composante maxwellienne de la population électronique, avec une température électronique moindre.

88

ESA SN-124
Agence Spatiale Européenne
KIST, R. (Institut f. Phys. Weltraumforschung, Freiburg)
Le gaz carbonique comme source de plasmas au laboratoire.
Septembre 1976
iv + 20 pages, 16 figures. En anglais.

Des mesures ont été faites à l'aide d'une sonde HF, d'un analyseur à potentiel de freinage et d'un spectromètre de masse dans une enceinte à plasma en utilisant tour à tour du gaz carbonique, de l'azote, de l'argon et de l'hélium afin de comparer les caractéristiques de ces divers gaz pour l'obtention de plasmas en laboratoire. Dans l'ensemble, on constate que le gaz carbonique donne de plus fortes densités de plasma à de plus faibles pressions de gaz neutre en même temps qu'une plus grande composante maxwellienne de la population électronique, avec une température électronique moindre.

88

CARBON DIOXIDE AS WORKING GAS FOR LABORATORY PLASMAS

by

R. Kist

Institut für Physicalische Weltraum forschung

Freiburg, West Germany

(The work described in this report was performed during the author's tenure of an ESRO External Fellowship at the University of Texas in 1974).

EUROPEAN SPACE AGENCY

AGENCE SPATIALE EUROPEENNE

114, avenue Charles de Gaulle, 92522-Neuilly, France

761520

TABLE OF CONTENTS

LIST OF FIGURES

CARBON DIOXIDE AS WORKING GAS FOR LABORATORY PLASMAS

ABSTRACT

Measurements with a RF probe, retarding potential analyser and mass spectrometer in a laboratory plasma tank have been performed using the gases CO_2, N_2, A and He in order to compare their properties as working gases for laboratory plasma production. The overall result is that CO_2 leads to higher plasma densities at lower neutral-gas pressures as well as to a larger Maxwellian component of the electron population, while the electron temperature is lower than that when N_2, A and He are used.

1. INTRODUCTION

One of the tasks involved in a laboratory plasma-diagnostics project at the University of Texas at Dallas (UTD) was to equip a cylindrical vacuum chamber, 70 cm long and 50 cm in diameter, with a plasma source providing a collisionless plasma with a Maxwellian, low-temperature velocity distribution of the electrons. To each end flange of the tank was attached a bell jar, as sketched in Figure 1. The general concept is to produce a primary plasma

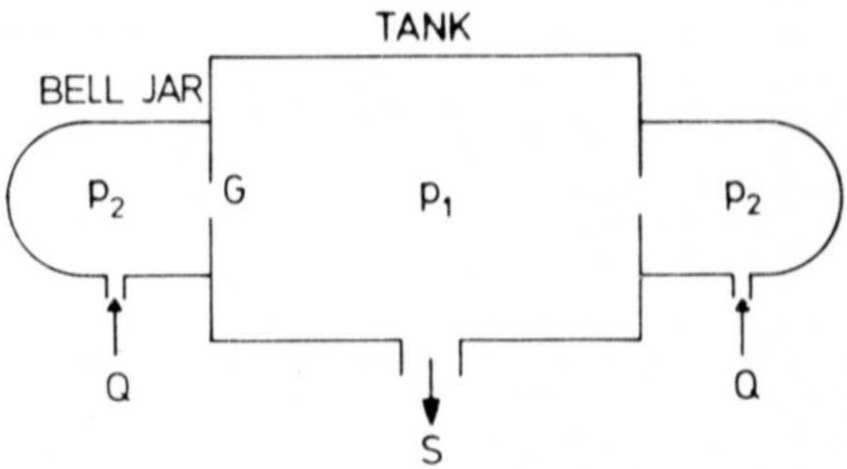

Figure 1. Schematics of the vacuum system.

(discharge) in a region of high pressure (bell jar) and let it expand through an orifice into a region of low pressure (tank). The present scientific note is concerned with the preparatory phase of the project in which different gases (CO_2, N_2, A, He) were compared in order to learn about their properties as working gases for laboratory plasmas.

2. GENERAL CONSIDERATIONS

The pressure p_1 and p_2 in the tank and bell jar, respectively, are governed by the following equations (see Fig. 1):

$$p_1 = \frac{2Q}{S} \tag{1}$$

$$\Delta p = p_2 - p_1 = \frac{Q}{G} \tag{2}$$

$$p_2 = Q\left(\frac{2}{S} + \frac{1}{G}\right) \tag{3}$$

Q is the gas stream in Torr l s^{-1} introduced into each bell jar, G is the gas kinetic conductivity in l s^{-1} of the orifice and S is the pumping speed in l s^{-1} applied to the tank. For $S>>G$ we get $p_2 \approx Q/G \doteq \Delta p$, i.e. $p_1 << p_2$. The first problem is to produce values for p_1 and p_2 such that p_2 is sufficiently high to run a discharge and p_1 is sufficiently low to allow for a collisionless plasma in the tank. 'Collisionless' means that there are practically no collisions between electrons and neutral gas particles. The collision frequency ν_{coll} then is governed by collisions with the tank walls according to

$$\nu_{coll} \cong \frac{V_e}{D} \tag{4}$$

where D is essentially the diameter of the tank and V_e is the mean velocity of the electrons.

The plasma density N_e in the tank is governed by the continuity equation

$$\frac{\partial N_e}{\partial t} = P - L \tag{5}$$

The production term P describes the quantity of electrons that enter the tank per unit time through the orifice. It is a complicated function of the discharge parameters such as working gas, working pressure p_2, geometry, material and voltages of electrodes (cathode, anode, grids) etc.

The loss term L describes the quantity of electrons that get lost per unit time primarily due

to recombination at the wall. In a very general way L can be described in terms of a mean lifetime τ_e that is spent by an electron in the tank before getting lost:

$$L \sim \frac{N_e}{\tau_e}$$

In a stationary-state situation ($(\partial N_e/\partial t) = 0$) the electron density in the tank will then be controlled by the production term P and the mean lifetime according to

$$N_e \sim P \cdot \tau_e \tag{6}$$

The lifetime τ_e will be closely related to the lifetime τ_i of the ions, since, owing to their low mass and the strong Coulomb forces, the electrons will always be tied to the ions in such a way that the plasma remains quasineutral. If ions get lost quickly (low τ_i), electrons will immediately get lost at a corresponding rate (low τ_e). Thus it is to be expected that τ_i and hence τ_e will decrease when the pressure p_1 is decreased, since at low pressure (below $\approx 10^{-2}$ pascal*) ions will travel directly to the wall, whereas at higher pressures p_1 they collide with neutrals, which leads to a long total ion path before the wall is reached. Collisions of electrons with the wall do not necessarily mean electron loss, since many electrons are reflected back by the potential within the ion sheath. As long as high plasma bulk velocities (wake phenomena) and/or magnetic fields (Lorentz forces) are not involved, the plasma potential with respect to the wall always attains a value such that the mean lifetime of the electrons matches that of the ions. Then the plasma body is quasineutral, and potential differences are confined to surface sheaths, the thickness of which is of the order of several Debye lengths.

According to equation (6) a decrease in the charged-particle lifetime must be compensated for by the provision of a sufficiently high production rate P to maintain a required plasma density.

3. CONSIDERATIONS CONCERNING CO_2 AS WORKING GAS

3.1 VACUUM PHYSICAL CONSIDERATIONS

The demand for a large pressure difference $p_2 - p_1$, p_2 typically being 1 pascal and p_1 less than 10^{-2} pascal, led to a required pumping speed S in the order of a few 10^3 l s^{-1}, a much higher value than the available turbomolecular pump could provide (only 260 l s^{-1}). In order to

* 1 pascal $\approx 10^{-2}$ Torr = 10 μmHg

reach the required pumping speed at relatively low cost, cryogenic pumping with liquid nitrogen seemed to be appropriate.

This vacuum physical requirement called for a working gas with a vapour pressure less than about 10^{-3} pascal at 77 K. CO_2 appeared to be a suitable candidate, since its vapour pressure is 5×10^{-8} Torr.

3.2 BREAKDOWN VOLTAGE AND IONISATION PROBABILITY

In order to get a high production term P the working gas should have low breakdown voltage and high ionisation probability. Figure 2 shows the Paschen curve for CO_2 in comparison with several other gases. The distance d between cathode and anode for our system is typically 10^2 mm. With p_2 in the order of 1 pascal, the parameter $p \cdot d$ for our discharge will be somewhere around 1. Since the slope of the Paschen curve in this region is very steep, even a slight displacement with respect to another curve (compare for example CO_2 with air) leads to an appreciable decrease in the breakdown voltage.

As to the ionisation probability, Figure 3 shows that CO_2 can be expected to provide a higher discharge current for a given pressure than N_2 and A. As an example, electrons within the discharge avalanche with an energy of 15 eV would produce about 30 times more ionisation in CO_2 than in N_2 and A.

The richness of energy states (electronic, vibrational, rotational) of the CO_2 molecule should allow the discharge electrons to randomise their kinetic energy more quickly, i.e. over a shorter diffusion length, than would be possible for electrons in N_2, A or He.

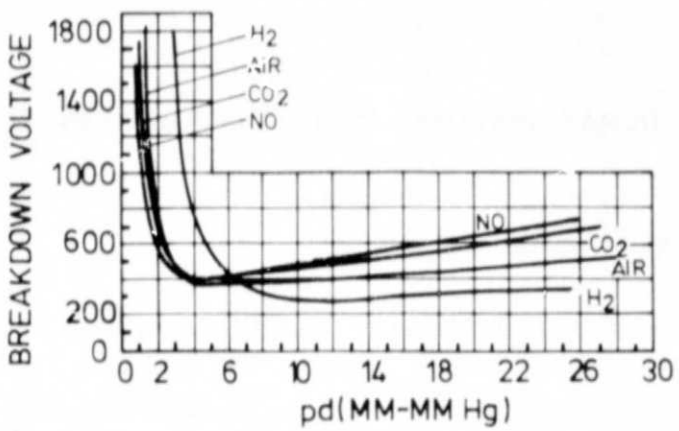

Figure 2. Paschen curves for various gases (after M. KNOLL, F. OLLENDORFF, and R. ROMPE, Gasentladungstabellen, Springer-Verlag, Berlin (1935)).

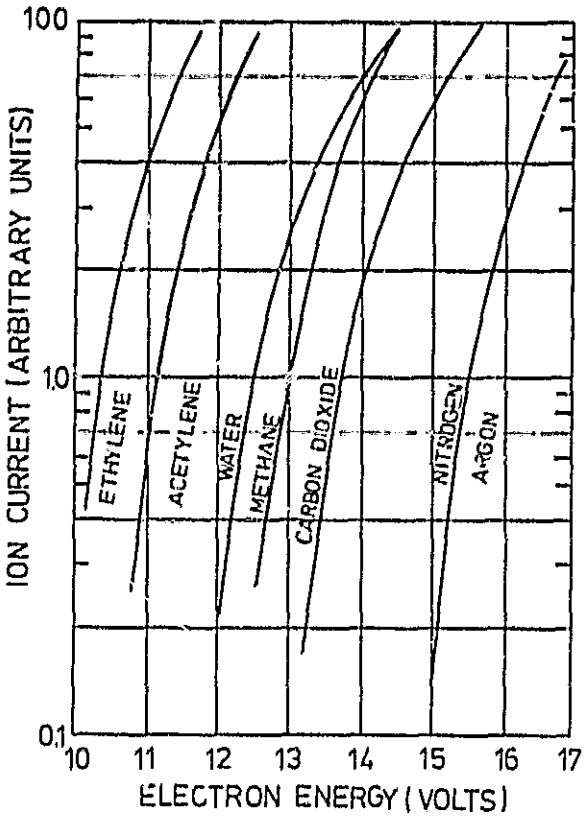

Figure 3. *Ionization probability for various gases (F.P. Lossing, A.W. Tickner, and W.A. Bryce, J. Chem. Phys. 19, 1254(1951)).*

3.3 RELEVANT REACTIONS OF CO_2

(a) Thermal dissociation: At 2000 K, 1.8 per cent of the CO_2 dissociates according to

$$2\,CO_2 \leftrightharpoons 2\,CO + O_2$$

The neutral gas temperature should stay far below 2000 K; it might approach about 1000 K in the vicinity of a heated cathode. Thus only a very low thermal dissociation rate is to be expected in the discharge.

(b) Reactions in the CO_2 discharge involving charged particles are as follows:

(1) Dissociative excitation

$$CO_2 + e \rightarrow CO^* + O' + e$$

$$CO_2 + e \rightarrow C^* + O' + O'' + e$$

(2) Ionisation

$$CO_2 + e \rightarrow CO_2^+ + 2e$$

(3) Dissociative recombination

$$CO_2^+ + e \rightarrow CO^* + O'$$

$$O_2^+ + e \rightarrow O^* + O'$$

(4) Charge exchange: $CO^+ + CO_2 \rightarrow CO + CO_2^+$ (very fast)

$$O + CO_2^+ \rightarrow O_2^+ + CO \rightarrow O^+ + CO_2$$

Little is known about the rate coefficients of these reactions.

(c) The consituents of the CO_2 plasma to be expected are listed below:

Neutrals	*Ions*
CO_2	CO_2^+
CO	CO^+
O_2	O_2^+
O	O^+
C	

The diagnostic investigations that were to be performed later in the plasma were concerned with the motion of plasma electrons (electromagnetic and electroacoustic plasma waves) so that the presence of different kinds of neutrals and ions was of no consequence as far as the interpretation of the measurements was concerned.

4. MEASUREMENTS

4.1 CRYOGENIC PUMPING OF CO_2

A preliminary investigation was made in order to determine the effect of a cryogenic type of pump on the tank pressure p_1 for various gases. For this purpose, a LN_2 cooled sorption pump was temporarily connected to the tank. Figure 4 shows its effect on p_1 for He, N_2 and CO_2. The effect is strongest for CO_2 and zero for He. Although in this case two effects were mixed, i.e. the absorption effect of the sieve material and the low temperature of the trapping

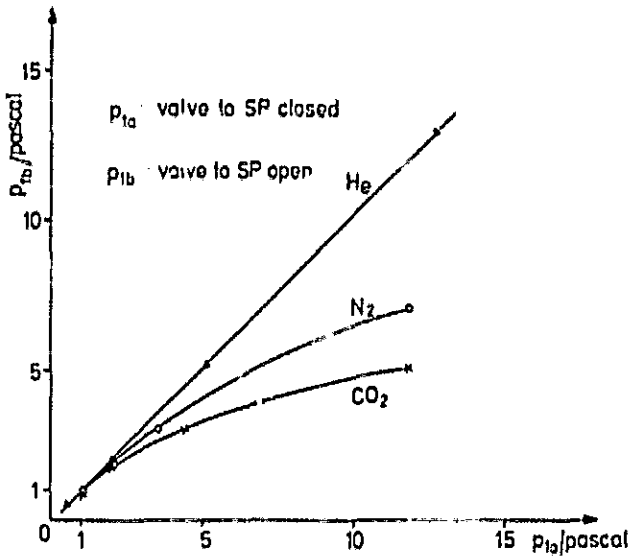

Figure 4. *Effects of sorption pump (SP) on the tank pressure p_1.*

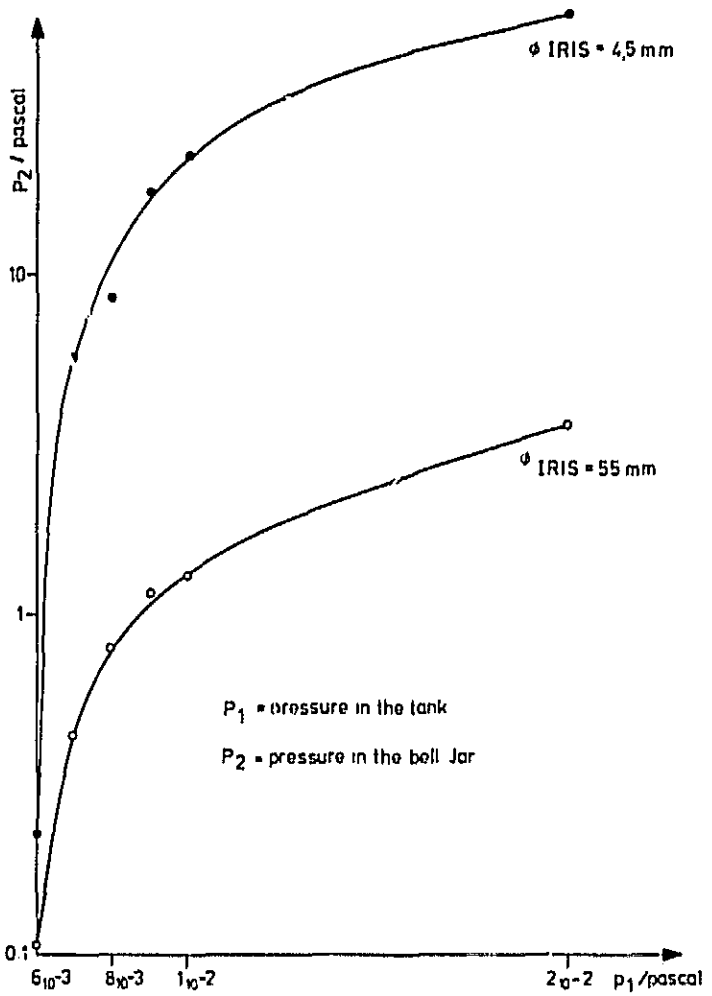

Figure 5. *CO_2-pressure in the tank for minimum and maximum setting of the iris diaphragm applying cryogenic pumping at LN_2 temperature.*

surface, it was to be expected that, with CO_2 as working gas, operation of a cryogenic wall would lead to a considerably higher pumping speed than if the turbomolecular pump were operated alone.

A copper shroud with copper tubes soldered on one side and covering about half the inner wall of the tank was inserted into the chamber. It could be cooled down to LN_2 temperature within about one hour. In addition to the cryogenic wall, an iris diaphragm was installed between bell jar and tank to provide a variable diameter of the orifice between the discharge and the measuring volume. As can be seen from Figure 5, it was possible to maintain a pressure ratio p_2/p_1 of roughly two to three orders of magnitude by adjusting the iris diaphragm and cooling the cryogenic wall down to liquid nitrogen temperature. Thus the vacuum requirements for producing a collisionless plasma were met by this device, using CO_2 as working gas.

4.2 BREAKDOWN VOLTAGE

Figure 6 shows measured values of the breakdown voltage (cold cathode discharge) as a function of pressure for a fixed distance d between cathode and anode (both of circular shape). The breakdown at pressures below about 2 pascal occurs at considerably lower voltages in CO_2 than in N_2. This is in agreement with the Paschen curves in Figure 2, it being expected that air would behave in a similar fashion to N_2.

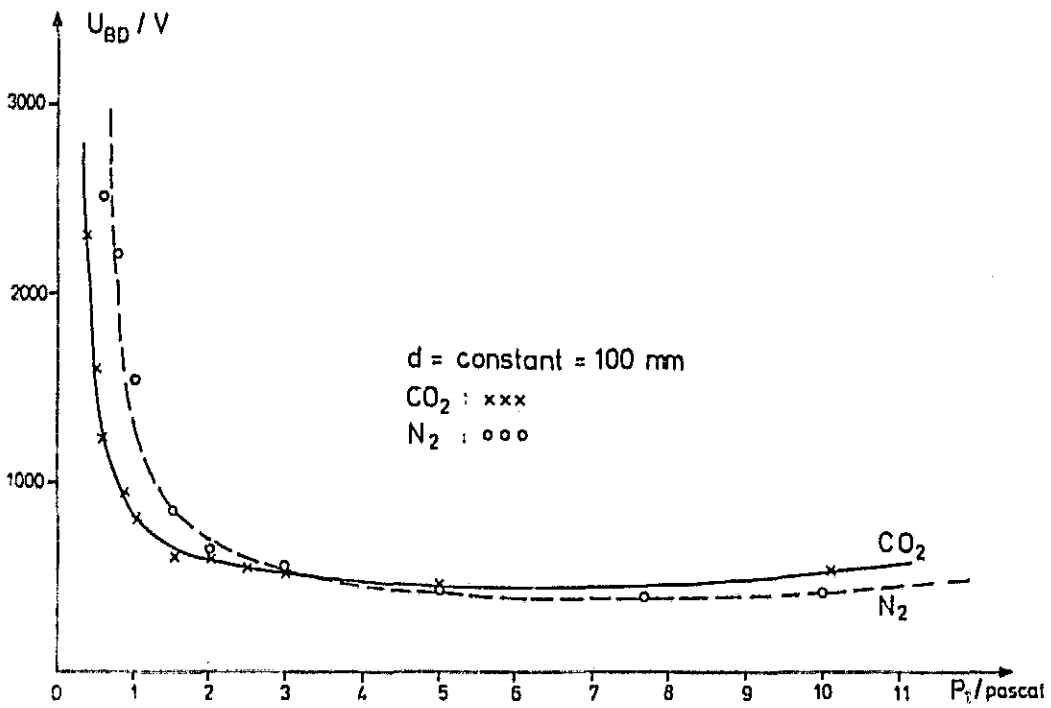

Figure 6. Breakdown voltage U_{BD} as a function of pressure p_1 for CO_2 and N_2.

4.3 ELECTRON DENSITY

To investigate further the properties of CO_2 as a working gas for plasma production, voltage current (U/I) characteristics were measured with a retarding potential analyser (RPA) in plasmas of CO_2, N_2, A and He. RPA measurements were performed over a pressure interval 0.5 to 10 pascal (without cryogenic pumping) and a discharge voltage range 600 V $\leqslant U_{DC} \leqslant$ 3000 V. In these cases p_2 is very close to p_1. A representative set of these characteristics is shown in the Figures 7 (a) through (d). The plot is semilogarithmic. Note the different scale for the log I ordinates. Although the discharge parameters (pressure p_1; discharge voltage U_{DC}) are not the same for the four curves they clearly show that in the CO_2 plasma both the strongest Maxwellian component and the lowest electron temperature T_e are obtained. The electron saturation current I_{sat} (defined here as the current at $U = +1$ V) of the RPA characteristics can be taken as a measure of the electron density obtained in the tank. Figure 8 (a) shows Log (I_{sat}) versus discharge voltage U_{DC} for CO_2, N_2 and A. Although the pressure for the CO_2 curve is lower (0.6 pascal) than the one for the N_2 and A curves (1.0 and 1.4 pascal, respectively) the saturation current for CO_2 is considerably higher than that for the other two gases. This holds over the entire range of U_{DC}.

Figure 8(b) shows Log (I_{sat}) as a function of pressure p_1 for $U_{DC} = 1200$ V. It can be seen that the value of I_{sat} is much higher for CO_2 than for N_2 and A in the pressure range below about 3.5 pascal. At higher pressures the density provided by a CO_2 discharge goes down. This fact may be due to volume recombination and/or formation of negative ions (CO_2^-). No detailed interpretation of this fact has been attempted since the pressures p_1 we deal with later are well below 3.5 pascal.

Simultaneously with the RPA-measurements, the parallel resonance frequency F_p of a cylindrical RF probe immersed in the plasma was measured. F_p is identified as the plasma frequency F_N (neglecting corrections for the collisions) which is related to the plasma density N_e according to:

$$N_e\ [m^{-3}] = 1.2456 \times 10^{10}\ F_N^2\ [MHz] \qquad (7)$$

Figure 9 shows F_N as a function of the discharge voltage U_{DC} comparing CO_2 with N_2 at pressures p_1 of about 0.6, 1.0 and 2.0 pascal. This diagram again shows the striking advantage of CO_2 for providing a large production term P for the steady-state plasma in the tank.

4.4 ELECTRON-ENERGY DISTRIBUTION

Returning to the set of RPA measurements, we find a further way of presenting the data that reveals facts again favouring CO_2 for plasma production. In general, most of the RPA

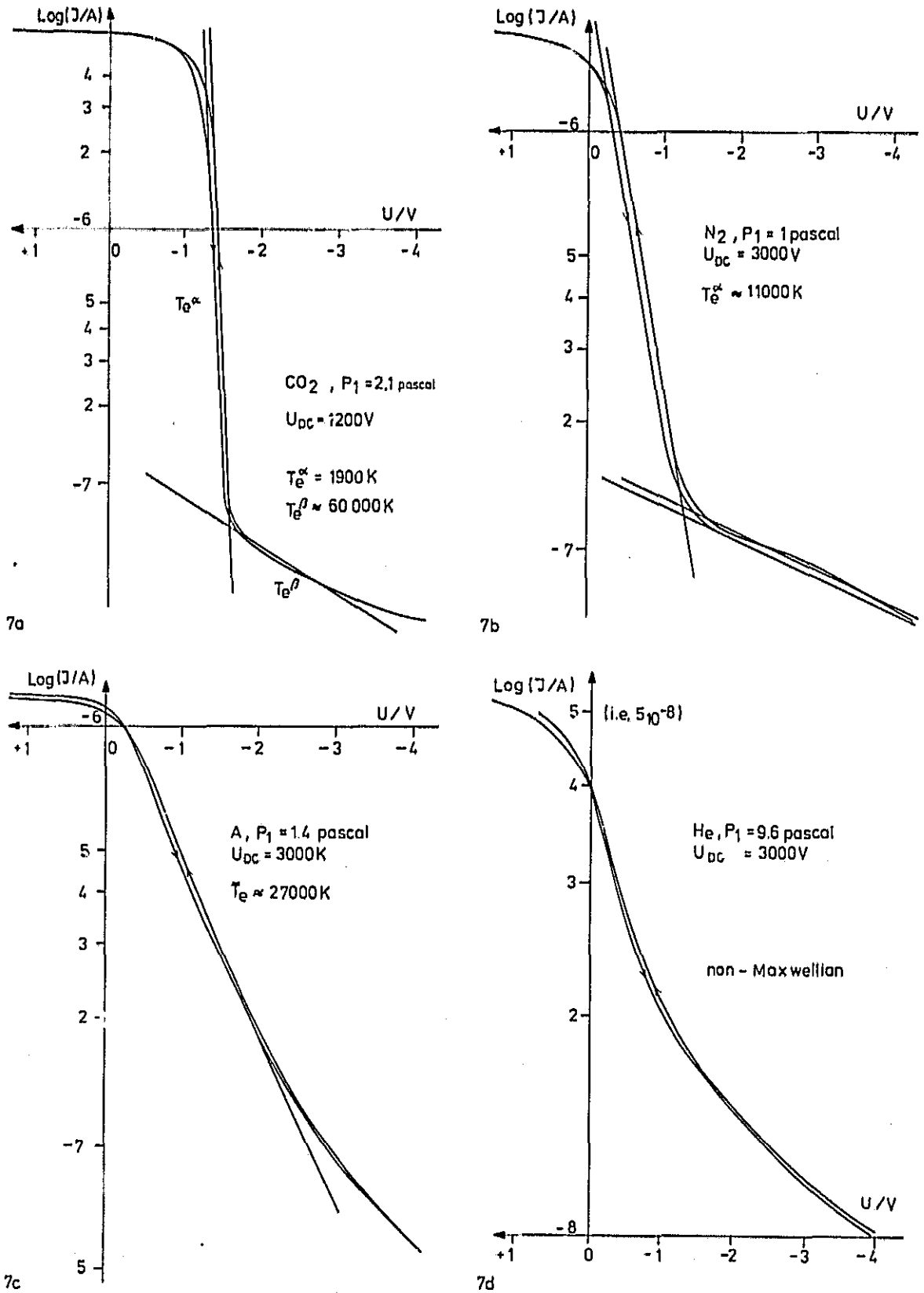

Figure 7. *Current/voltage characteristics obtained with the RPA in CO_2 (a) N_2 (b), A (c), and He (d).*

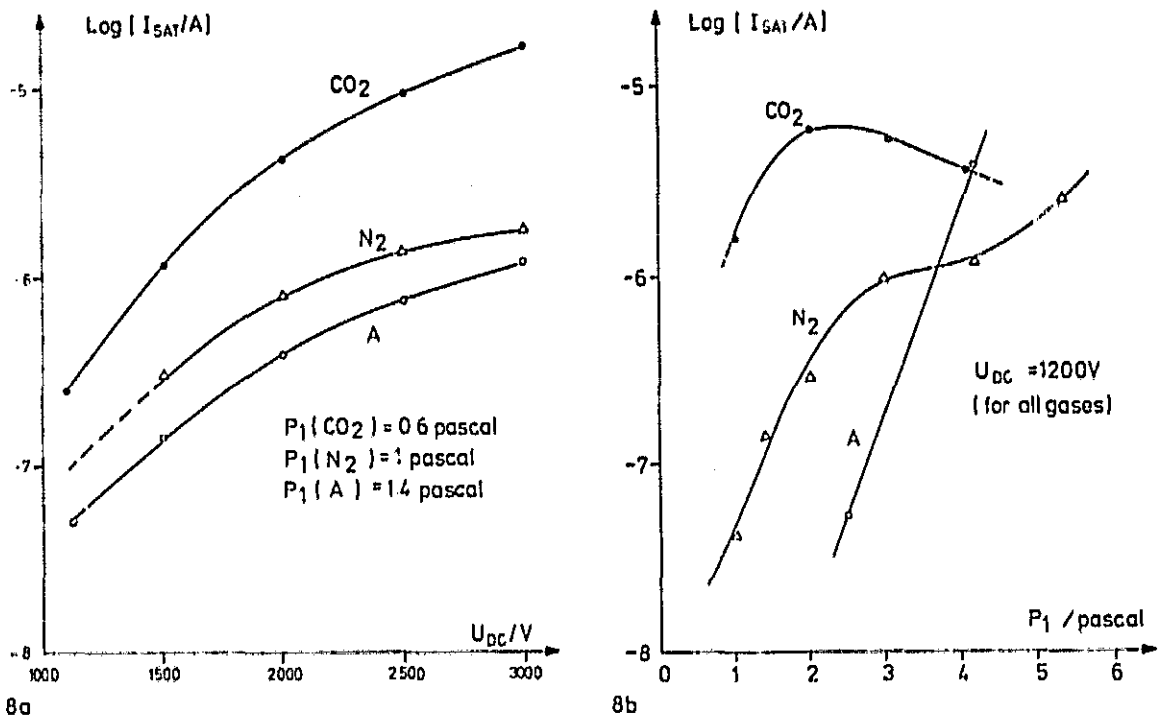

Figure 8. *(a) Saturation current I_{sat} taken from RPA curves versus cold cathode discharge voltage U_{DC} (with neutral gas pressure approximately constant) for CO_2, N_2 and A. (b) Saturation current I_{sat} taken from RPA curves versus neutral gas pressure p_1 (constant discharge voltage U_{DC}) for CO_2, N_2 and A.*

characteristics measured in CO_2 and N_2 plasmas have the general form shown in Figure 10. The semilogarithmic plot usually contains three components (α, β and γ) of the electron population represented by straight or nearly straight lines which can be attributed to electron temperatures T_e^{α}, T_e^{β}, T_e^{γ}, respectively. Figures 11 (a) and (b) represent these temperatures (T_e^{γ} only as table) as a function of both p_1 and U_{DC}. The scale for T_e^{α} is on the left, the scale for T_e^{β} on the right side of the diagrams.

The representation shows the following points:

(1) T_e^{α} (CO_2) stays low (1000 to 3000 K) over the investigated ranges of p_1 and U_{DC}, respectively.

(2) T_e^{α} (N_2) rises strongly towards the 10^4 K range when the pressure decreases to 1 pascal. For constant pressure (1 pascal) it is about 10^4 K and rises slightly with increasing discharge voltage U_{DC}.

(3) T_e^{β} (CO_2) increases with increasing pressure for constant U_{DC} (1200 V) and decreases with increasing U_{DC} at constant pressure (0.6 pascal) towards a constant level (about 3×10^4 K).

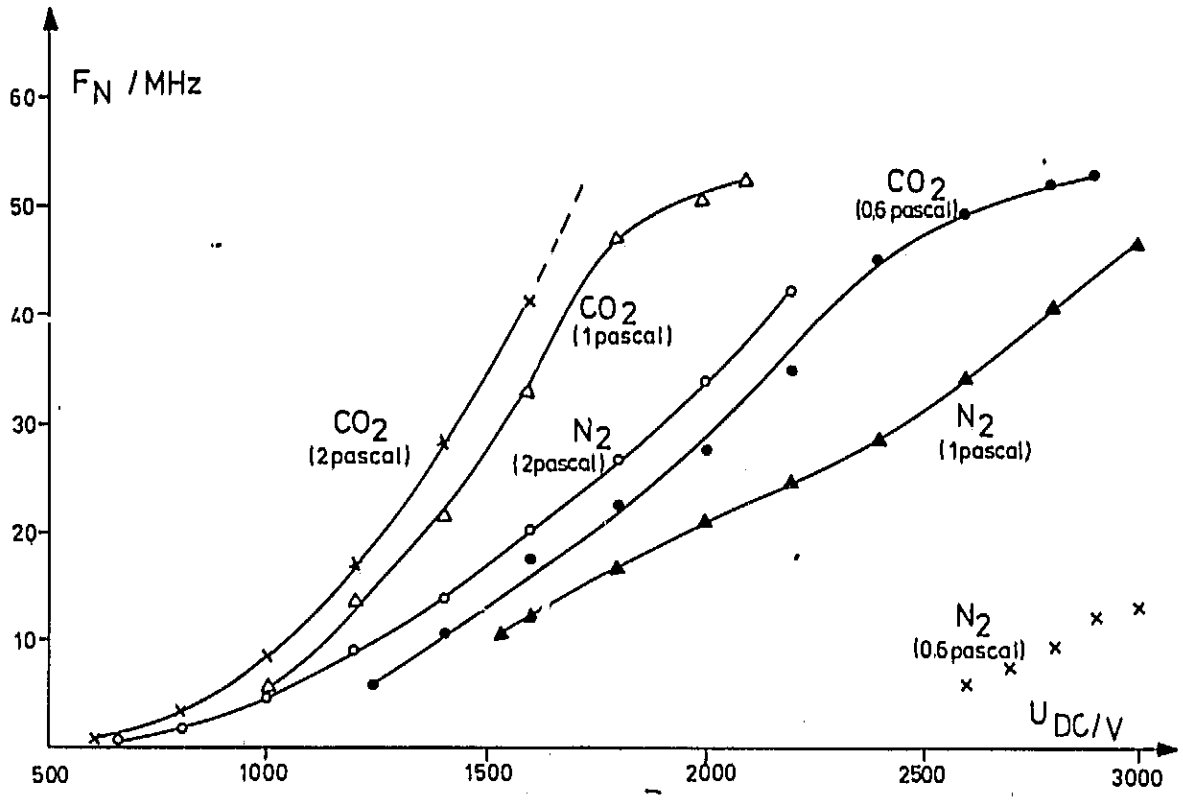

Figure 9. *Plasma frequency f_N in the tank as a function of discharge voltage U_{DC} for CO_2 and N_2 at three different neutral gas pressures p_1.*

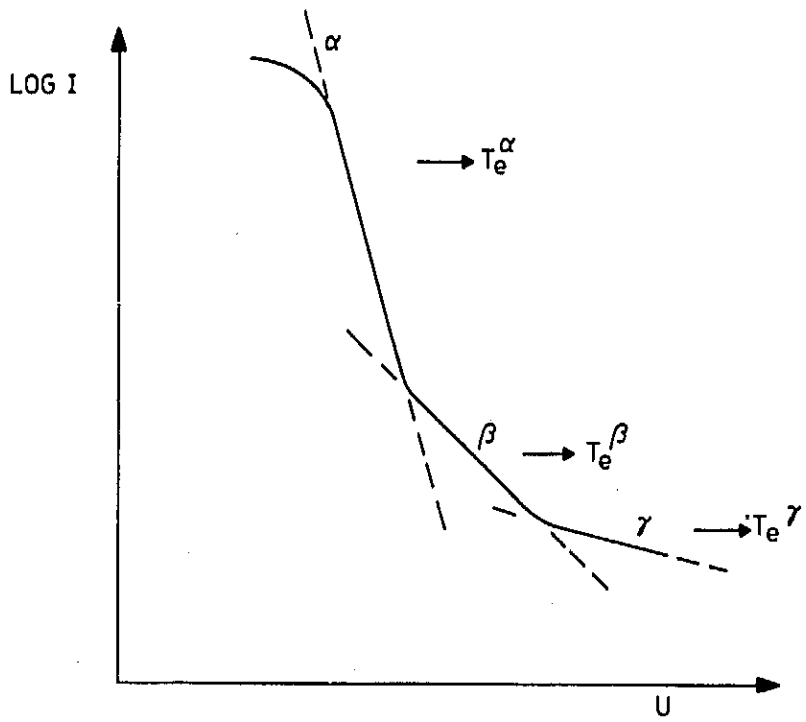

Figure 10. *General three-component feature of the I/U characteristic as seen with the RPA in CO_2 and N_2.*

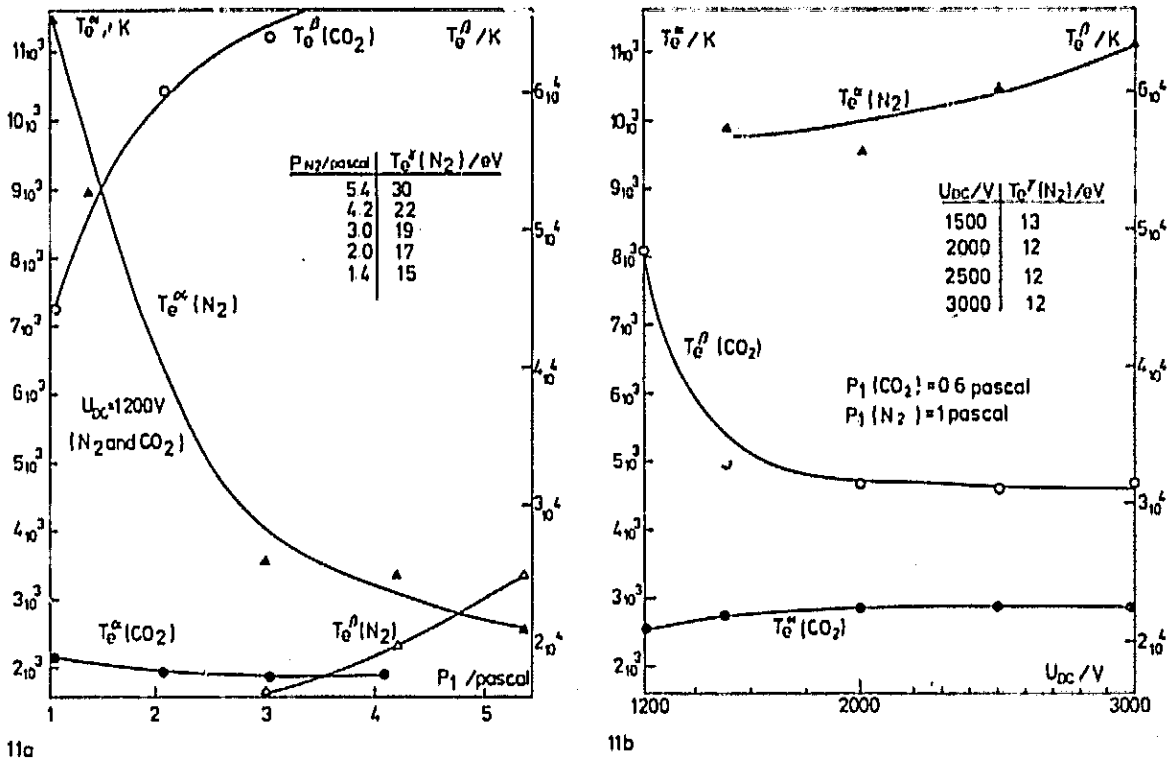

Figure 11. *(a) Temperature components T_e^α and T_e^β versus pressure p_1 for CO_2 and N_2 at constant discharge voltage U_{DC}. (b) Temperature components T_e^α and T_e^β versus discharge voltage U_{DC} for CO_2 and N_2 at constant pressure p_1. T_e^β for N_2 is not included, since the β-component could not be identified clearly enough from the I/U characteristics.*

(4) T_e^β (N_2) is low compared with T_e^β (CO_2) and rises slowly with increasing pressure.

4.5 THE FINAL LABORATORY PLASMA SYSTEM

The body of information collected by the measurements described above clearly favoured the choice of CO_2 as a suitable working gas for producing a laboratory plasma with a strong Maxwellian electron component of low temperature (a few thousand K). A source which was then developed was of the back diffusion type, making use of a heated cathode in order to further increase the production rate P. The final system is shown in Figure 12. The brush electrode was used temporarily for cold cathode discharge experiments and acted later as the anode for the back diffusion source. The paddle proved very effective in baffling high-energy electrons. The drawing also shows schematically the position and geometry of the diagnostic probes as well as the LN_2-cooled copper shroud for cryogenic pumping. A screen was present in the chamber. This was occasionally used to influence the plasma potential by having a bias voltage applied to it, but in general it was kept at floating potential. Typical neutral-pressure values for this laboratory plasma system in operation were a few pascal in the discharge region (bell jar) and 10^{-2} pascal in the tank.

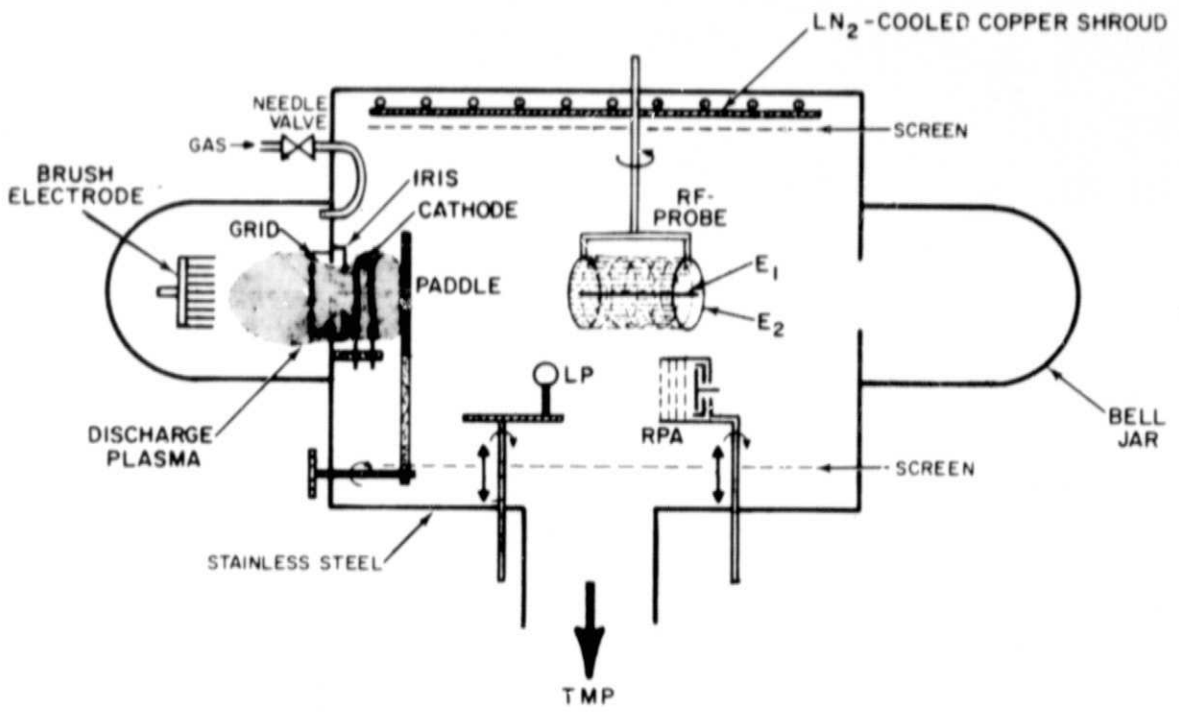

Figure 12. Laboratory plasma system with plasma source and diagnostic probes.

4.6 PLASMA DIAGNOSTIC-PROBE MEASUREMENTS

RF-measurements were performed with a cylindrical two-electrode system (E_1, E_2), as shown in Figure 13. The principle of the RF-measurement is also shown. A swept-frequency RF generator provides a signal of constant amplitude within the frequency interval of typically 1 to 25 MHz. Both the RF-reference voltage $\underline{U}_R$ at E_1 and the test voltage $\underline{U}_T$ at E_2 are measured and compared as to their complex ratio

$$\underline{U}_T/\underline{U}_R = E + jF$$

by means of a network analyser (hp 8407).

The signals provided by the network analyser are magnitude

$$a = \left|\frac{\underline{U}_T}{\underline{U}_R}\right| = \sqrt{E^2 + F^2} \qquad [\text{dB}]$$

and phase φ = arctan (F/E) in degrees. Magnitude and phase together are a measure of the complex plasma impedance $Z = X + jY$ between E_1 and E_2.

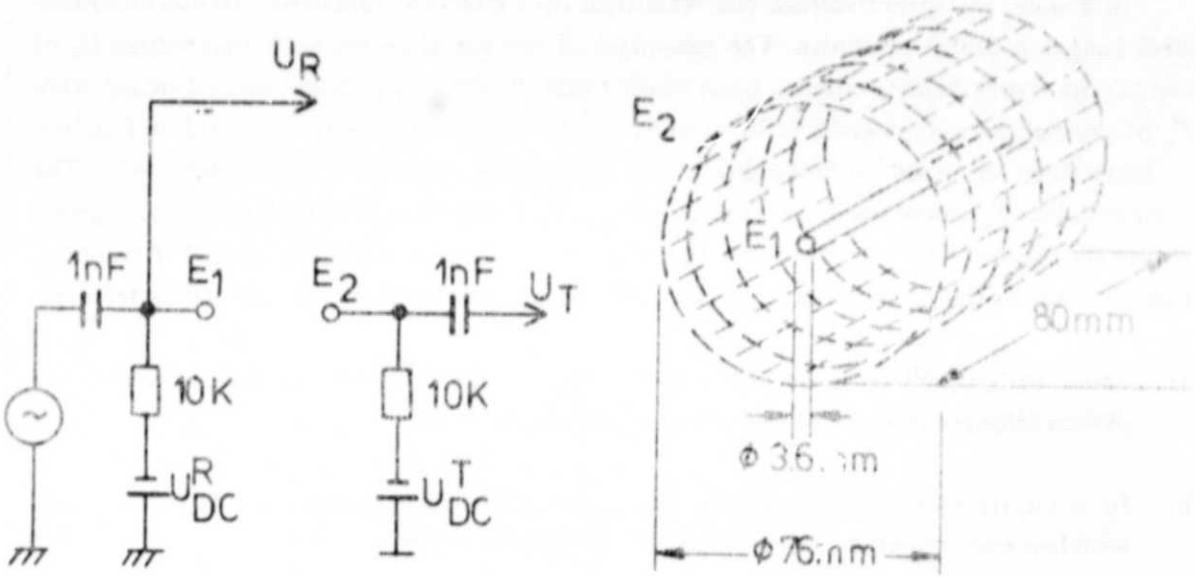

Figure 13. *Cylindrical RF-probe and principle of RF impedance measurement.*

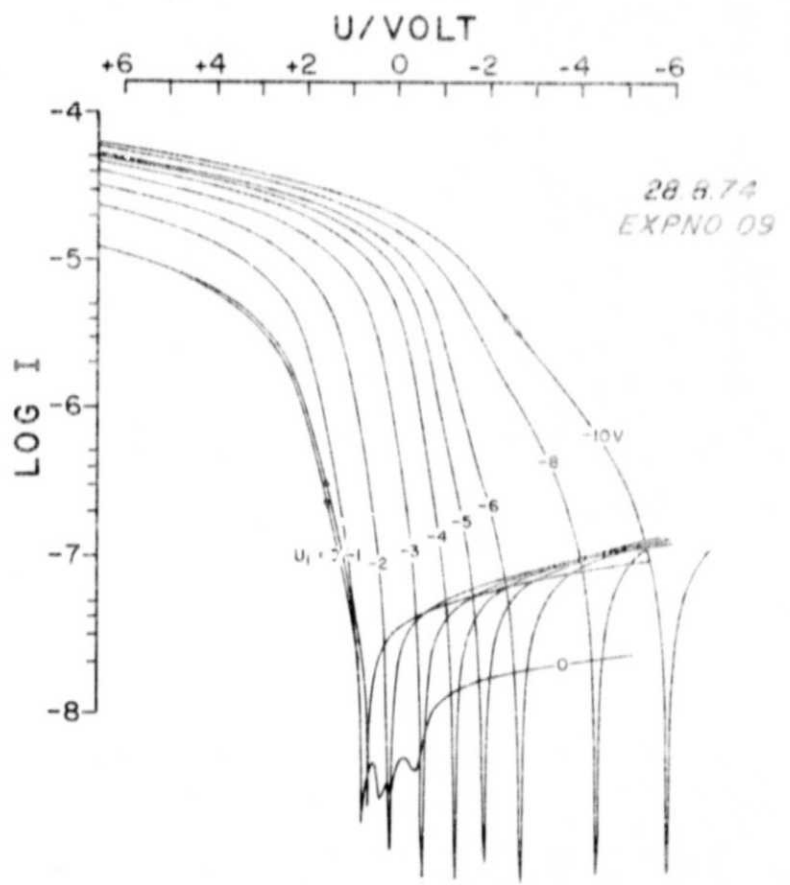

Figure 14. *Langmuir characteristics for various values of the bias voltage U_1 of the plasma-source heating circuit.*

In Figure 14 current/voltage characteristics of a spherical (diameter: 10 mm) stainless-steel Langmuir probe are shown. The parameter of this set of curves is the bias voltage U_1 of the plasma source heating circuit. It can be seen that the velocity distribution and temperature T_e of the electrons is markedly influenced by U_1. In the present case the distribution function is Maxwellian in good approximation for U_1 values of -2 V, -3 V and -4 V. The corresponding T_e values are 0.55, 0.53 and 0.52 eV, respectively. For each of these Langmuir curves the magnitude a measured as a function of frequency was plotted on an X-Y recorder. Figure 15 shows the corresponding set of curves, which reveals the following essential features:

a) above the parallel resonance f_P, which is in our case (no magnetic field) equal to the plasma frequency f_N, an additional resonance f_Z occurs and

b) f_Z is clearly most pronounced for the case of Maxwellian distribution of the electrons with low electron temperature T_e ($U_1 = -2$ V, -3 V, -4 V).

This resonance f_Z can be understood in terms of resonantly excited electroacoustic waves (also called electron-pressure or Landau waves). These waves are set up by an RF source above

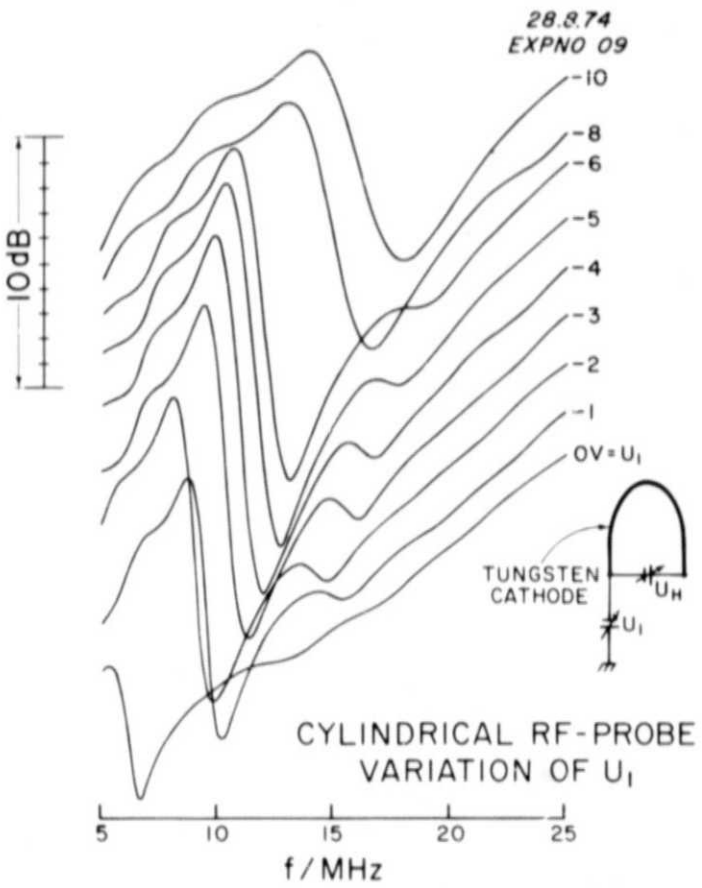

Figure 15. Plasma impedance magnitude of the cylindrical two-electrode system.

the plasma frequency. Excitation of this longitudinal type of plasma wave, which is damped with increasing frequency by collisionless or Landau damping, is predominantly responsible for the real part of the impedance of an electrode system immersed in a plasma. For a single electrode this real part would decrease monotonically with increasing frequency. For a two-electrode system (E_1, E_2), as used in our experiment, however, a characteristic electrode distance d can be defined (distance between inner and outer cylinder). In this case the electroacoustic wave can produce a standing-wave pattern between E_1 and E_2. This is expected to occur essentially at eigenfrequencies of the system (electrodes/plasma) for which the wavelength λ_{ea} (or integer multiples of it) matches the distance d. The detailed discussion of these resonances is outside the scope of the present paper.

4.7 MASS-SPECTROMETER MEASUREMENTS

As regards the chemical composition of the CO_2-plasma, measurements with a magnetic-deflection neutral mass spectrometer (a laboratory model of the Lunar Atmospheric Composition Experiment (LACE) flown to the moon by APOLLO 17 – J. Hoffman, principal investigator) provided information about the abundant neutral molecules and atoms. The neutrals entering the ion source of the mass spectrometer are ionised by an electron beam. The ions are accelerated and collimated to a beam which passes into a magnetic analyser by which the ions are separated according to their momenta and detected in one of three mass channels.

Figures 16 (a) and (b) show a set of measured mass spectra (signal current versus amu number) for two energies E_e of the ionising electron beam (25 and 90 eV, respectively). The sequence of the measuring conditions in each case is

(a) background gas at 9×10^{-5} pascal, with no CO_2 introduced via bell jar and no plasma;
(b) CO_2-pressure at 2×10^{-3} pascal, but plasma switched off;
(c) CO_2-gas stream as in (b), but with plasma switched on.

In case (c) the neutral gas pressure increases by about one order of magnitude, mainly because CO, which is produced by dissociation in the discharge, cannot be pumped cryogenically at LN_2 temperature. The pressure increase was measured independently by an ionisation manometer in the tank and by a Penning manometer within the mass spectrometer. As a result of this pressure increase, the base line of the spectrogram is enhanced and (owing to multiple scattering in the ion source) the line width of the detected peaks is increased (which affects the amu selectivity of the instrument).

The spectra in Figure 16 (a) and (b) show the following features:

1. When the plasma is switched on, the CO and O_2 peaks strongly increase; CO becomes the dominant molecule. This holds for both electron energies (E_e = 25 and 90 eV). The

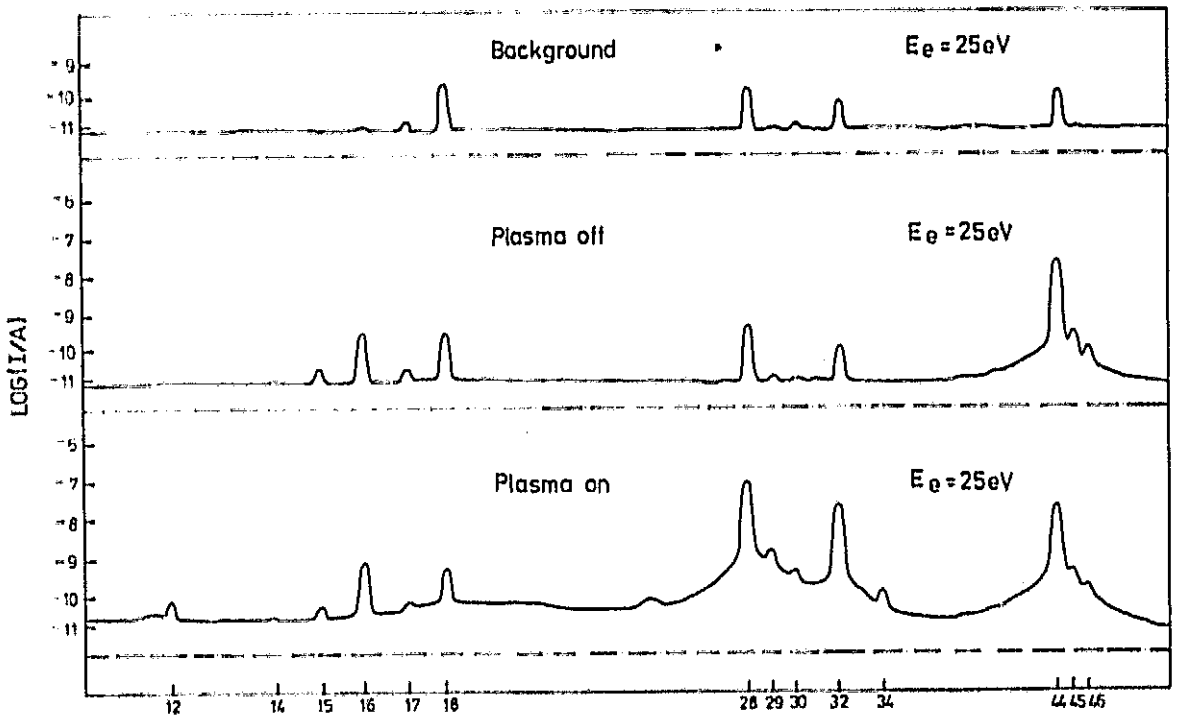

16a

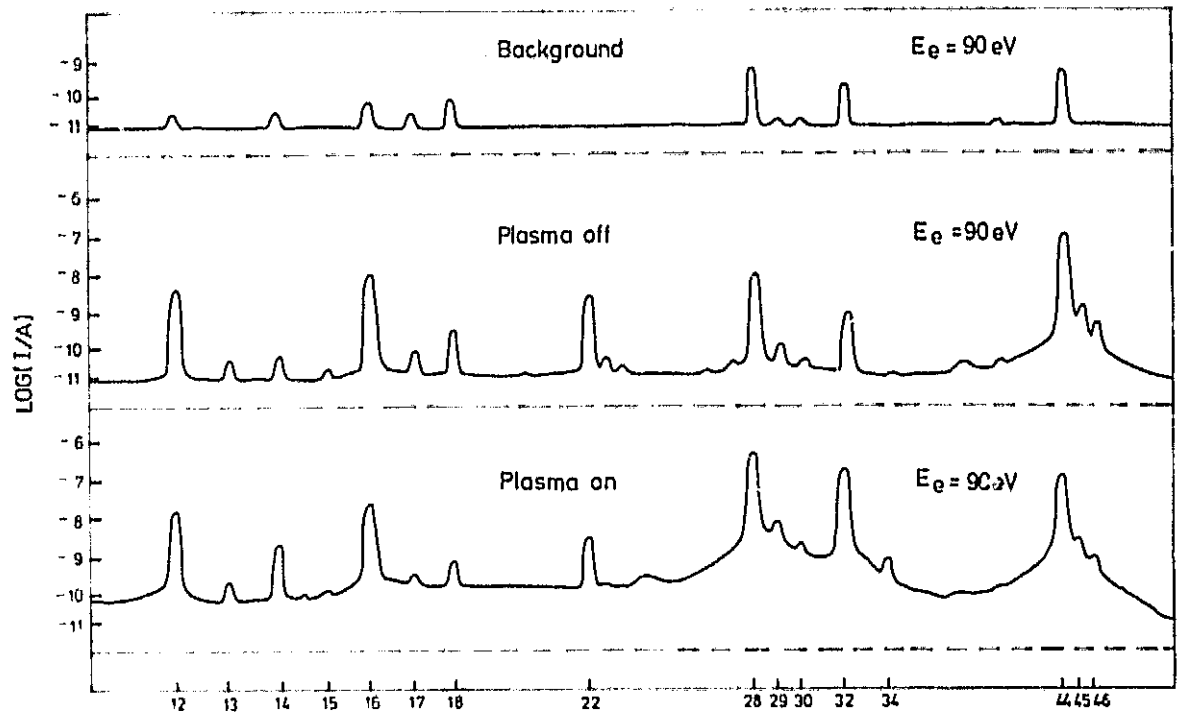

16b

Figure 16. *(a) Mass spectra with 25 V acceleration voltage applied to the electron beam of the ion source. (b) Mass spectra with 90 V acceleration voltage applied to the electron beam of the ion source.*

previously measured cracking pattern of the instrument for CO_2 (private communication by J. Hoffman) shows that only about 10% of the incoming CO_2 molecules are decomposed into CO and O in the ion source at E_e values of 70 . . . 90 eV. The strong enhancement of CO thus implies that dissociative excitation: $CO_2 + e \rightarrow CO^* + O' + e$ followed by $O + O \rightarrow O_2$, is a process which is very efficient in the CO_2 discharge. Since the neutral gas pressure in the discharge volume is in the order of 1 pascal, the density of the CO molecules coming from the discharge can exceed the CO_2 density in the tank because CO is not cryogenically pumped at LN_2 temperature.

2. For E_e = 25 eV and the plasma switched off (CO_2 pressure of the order of 10^{-3} pascal), no carbon ^{12}C is detected. This holds also for CO_2 pressures of 10^{-2} pascal without plasma (separate measurement). Thus the appearance of ^{12}C when the plasma is switched on indicates that ^{12}C is produced to a small extent in the discharge, according to the reaction $CO_2 + e \rightarrow C^+ + O' + O'' + e$.

   For E_e = 90 eV the ^{12}C peak is strongly enhanced. This is due to the dissociation of CO_2 by electron bombardment in the ion source of the mass spectrometer. According to the above-mentioned cracking pattern, about 9% of the CO_2 molecules will be cracked down to produce ^{12}C at these high values of E_e.

3. The CO_2 peak (amu = 44) is followed by two isotopic lines at amu = 45 and 46. These are due to the molecules $^{13}C\,^{16}O_2$ and $^{12}C\,^{16}O\,^{18}O$, respectively. The abundance – relative to CO_2 – of these isotopic molecules is about 1% and 4%. There are corresponding isotopic lines at amu = 29 and 30. These are related to $^{13}C\,^{16}O$ and $^{12}C\,^{18}O$, respectively.

4. The peak at amu = 18 is due to residual H_2O vapour present in the vacuum system; the mass 17 peak is produced by dissociative ionisation of H_2O in the ion source leading to OH^+.

5. At E_e = 90 eV, double ionisation of CO_2 is possible, leading to lines at amu = 22(CO_2^{++}), 22.5 ($^{13}C\,^{16}O_2^{++}$) and 23 ($^{12}C\,^{16}O\,^{18}O^{++}$).

5. CONCLUSIONS

The investigations reported here show that carbon dioxide has properties that favour it as working gas for the production of a collisionless Maxwellian plasma with low electron temperature (T_e in the order of ionospheric F-region values). CO_2 leads to higher plasma densities at lower pressures as well as a larger Maxwellian component of the electron popul-

ation with lower electron temperature as compared with other gases such as Ne, A, and He. The fact that CO_2 can be pumped at high pumping speeds by a liquid-nitrogen-cooled cryogenic wall enables a steep neutral gas pressure gradient to be achieved between the discharge volume and the measuring volume. However, in the diffusion type of plasma system used in the present work, the CO concentration relative to the CO_2 density is strongly increased in the tank because CO is not pumped cryogenically at LN_2 temperature. The abundance of oxygen in the plasma naturally imposes restrictions on the choice of materials for diagnostic probes etc.

It may finally be mentioned that studying CO_2 plasma in the laboratory may contribute to an understanding of some of the properties of the Martian and Venusian ionospheres.

ACKNOWLEDGEMENTS

The author expresses his gratitude to D. Winningham for providing the RPA-sensor, to J. Hoffmann for providing the mass spectrometer and to B. Milam for his engineering assistance. ance. Many thanks also go to W. Heikkila for his constant interest in this project and valuable discussions. The work described in this report was performed during the author's tenure of an ESRO External Fellowship at the University of Texas at Dallas 1974. The work represents part of a laboratory plasma project supported by NASA Headquarters Grant NGR 44-004-030.